



The quest for reference stations at the National Observatory of Athens, Greece

Olga-Joan Ktenidou¹, Antonia Papageorgiou¹², Erion-Vasilis Pikoulis¹², Spyros Liakopoulos¹, Fevronia Gkika¹, Ziya Cekinmez¹³, Panagiotis Savvaidis¹⁴, Kalliopi Fragouli¹⁵, Christos Evangelidis¹

5 ¹Institute of Geodynamics, National Observatory of Athens, Lofos Nymfon-Thisseion, Athens, 11850, Greece

²University of Patras, Patras, 26504, Greece

³National Technical University of Athens, Athens, 15780, Greece

⁴Aristotle University of Thessaloniki, Thessaloniki, 54124, Greece

⁵University of the Aegean, Mytilene, 22510, Greece

10

Correspondence to: Olga-Joan Ktenidou (olga.ktenidou@noa.gr)

Abstract. The assumption of reference station conditions is investigated for the first time across 60 rock stations belonging to the broadband and accelerometric networks of the National Observatory of Athens. We select the stations based on the established belief that they lie on rock, and provided that their data have been publicly available for long enough to yield a substantial number of recordings. No site effects studies have been conducted before for the ensemble of the stations under study. Furthermore, no ad hoc field campaigns have been performed to characterise them, save in few cases. The first step is to compile all existing information for these stations from all publicly available sources and past studies, including geology, topography, station installation, $V_{s,0}$ estimates and any other known metadata. The second step is to compile ad-hoc information from maps combined with the operator's first-hand experience of the sites, to better describe the geological unit and age, along with other characteristics such as station installation and morphology. The third and largest step is to compile the first Greek ground-motion dataset on rock and to perform a detailed analysis of the recordings to estimate site-specific transfer functions and hence assess local site response characteristics for each station. A strong-motion dataset of 6840 recordings is developed and curated for this purpose, visually inspected and processed in the time and frequency domains. Single-station amplification functions (horizontal-to-vertical spectral ratios, HVSR) are estimated from the seismic data, and the site resonance characteristics are assessed, not only in the conventional way of combining horizontal components, but also assessing the transfer function's directional sensitivity. Considering that 'true' reference site behaviour implies low, flat amplification with no directional dependence, these transfer function characteristics are combined with the compiled station metadata -existing and new- to evaluate the stations' overall capacity as reference sites. The stations are grouped in terms of behaviour and the preferred ones are recommended, hoping to facilitate the better use of seismic data in future hazard applications.

15
20
25
30



1 Introduction

The importance of understanding site conditions at strong-motion recording stations has been known for decades. Important global databases such as NGA-West2 (Ancheta et al., 2014) made a point of procuring rich and homogeneous station metadata in terms of Vs, depth to bedrock, etc. Ground motion models have moved towards more detailed descriptors of station conditions, and a global effort is being made in characterising stations. In recent years, particular importance has been attached to assessing ground motion on rock sites in particular, while in the past it was considered as rather homogeneous (some notable exceptions including the seminal works of Silva & Darragh 1995 and Steidl 1996). We now recognise that material properties and geometry –the main ingredients of site response- can cause ground motions to differ strongly between rock stations, and that they are not as ‘uninteresting’ as we once thought in terms of site response (i.e., the implicit assumption of negligible amplification does not hold). This has important potential impact on reference ground motions and the definition of reference stations, which once were simply defined as those coming from ‘rock’ sites. It has impacted seismic hazard and risk assessment for significant structures and critical infrastructures, which now often accounts in detail for such rock property variations. However, rock sites can be notoriously challenging to characterise, and many networks have not characterised their rock stations, as priority had been initially –and reasonably- given to stations lying on soils.

Some studies in the past decade or so attempted to focus on rock sites. Van Houtte et al. (2012) tested stations in Christchurch that were typically used as reference stations without previous checks, by computing site transfer functions. Ktenidou & Abrahamson (2016) found broadband amplifications even in CENA rock sites that had been considered as extremely hard (V_{S30} of 2000 m/s). More recently, much more systematic and large-scale efforts have been made on European level by Lanzano et al. (2020), who made a large-scale detailed effort for defining reference sites in Central Italy using various proxies as well as transfer functions from seismic data and noise, as did Pilz et al. (2020) who also included artificial intelligence tools in their reference site identification. Di Giulio et al. (2021) attempted to assess in a systematic way the seismic station characterisation efforts across Europe in terms of data quality, methodological reliability etc., emphasising the importance of consistency.

In Greece, whose seismic data are of great importance to European and even global ground-motion datasets, relatively little progress has been made so far in characterising stations. Many logistical reasons lie behind this, including the fact that a significant number of seismic networks are run by different operators exist (Evangeldis et al., 2021), there is a large number of stations off the mainland or in areas that are difficult to approach due to terrain, etc. Some efforts have been made to compile what station metadata exist, since the early days of HEAD, the first strong-motion database (Theodoulidis et al., 2004). Margaris et al. (2014) provided a brief history of the characterisation of Greek strong-motion stations with boreholes, geophysical campaigns and microtremors, while Stewart et al. (2014) compiled values of V_{S30} and other site descriptors for some strong-motion stations, mostly based on information within a 1-km radius from the stations per se. Margaris et al. (2021) include the most up-to-date version of available strong-motion station metadata, mostly through proxies. We note that the ensemble of stations considered in all the above studies includes a large number of stations that lie on soft ground, and a



large fraction of them are not yet publicly available through European waveform services (ESM). Only one systematic effort was made so far, for one of the Greek networks (HL, doi:10.7914/SN/HL) by Grendas et al. (2018), in which the actual strong-motion recordings were analysed to compute empirical transfer functions to understand site amplification; however, the majority of those stations are again not publicly available in terms of waveform data.

70 The goal of this work is to focus on the networks of the National Observatory of Athens (doi:10.7914/SN/HL), including not only the strong-motion one (<https://accelnet.gein.noa.gr>) but also the broadband seismic one (<https://bbnet.gein.noa.gr/HL/>), and further focus on the stations openly available in real-time continuous mode through the EIDA@NOA node (Evangelidis et al., 2021). For a fraction of the strong-motion stations, site conditions are known in great detail thanks to geophysical in situ investigations conducted in the recent national project HELPOS (Hellenic Plate Observing System); however, most of
75 these stations are either not open or lie on soils. To date, most of the openly available strong-motion stations are still characterized via proxies, while none of them have been analysed to determine empirical amplification functions (spectral ratios). Moreover, there has never been a systematic, consistent effort to include broadband stations as well, despite the increasing importance that is recently being attached to broadband data in ground-motion databases. In the HL networks, only a few small-scale efforts were made in the recent past to understand the behaviour of selected strong-motion and
80 broadband stations using the recordings themselves (Ktenidou & Kalogeras, 2019; Ktenidou et al., 2021a, 2021b). These were made using only limited datasets, mostly as proof of concept to the work at hand. This paper marks the beginning of a more systematic study of the NOA network conditions, starting with rock sites.

2 Strong-motion data and analysis

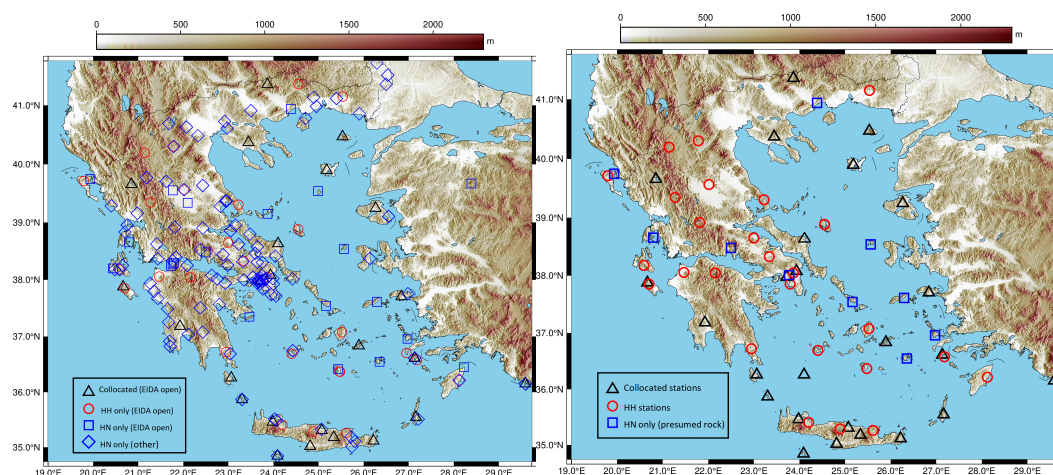
2.1 Station and data selection

85 All stand-alone broadband stations (HH channels) and collocated broadband and strong-motion stations (HH and HN channels) are generally thought to lie on rock conditions. Hence all such stations are included in this study, as long as they had enough recordings at the end of 2021, which could be publicly accessible via the EIDA@NOA node at that time (Evangelidis et al., 2021). In addition, stand-alone strong-motion stations (HN) open to the public via EIDA were considered, and those thought to lie on rock were selected. The layout of the stations selected is shown in Fig. 1b, and some
90 basic information about them is compiled in Table 1 (where ‘HNC’ indicates strong-motions stations installed at the same site as a broadband station).

A threshold minimum magnitude of ML4 was considered for each station, dropping down to M3.5 only in one case, for a station installed in 2021. The maximum distances considered varied according to noise level and station population of recordings, but scaled from out to 150 km for smaller events and out to 300 km or more for large events. The overall M-R
95 distribution is shown in Fig. 2 for the ensemble dataset, and can be found on a station-specific basis in the Supplement (Figs S1 and S2). Because the purpose of this dataset is the study of site effects (not, for instance, the development of ground motion models) and the M-R distributions are used as an indication only, we use local magnitude scale and epicentral



distance metrics and do not go into the details of moment magnitude and rupture distance for the large events in the dataset. A total of 6840 recordings are analysed in this study. The number of records per station is shown in Fig. 2b. The minimum number of usable recordings for the single least populated station is 8, the mean number of recordings is 90, while some stations have more than 300.



105 **Figure 1:** a. Map of all HL stations in the end of 2021. b. Map of selected stations (believed to lie on rock, with publicly available data via EIDA@NOA and adequate number of events).

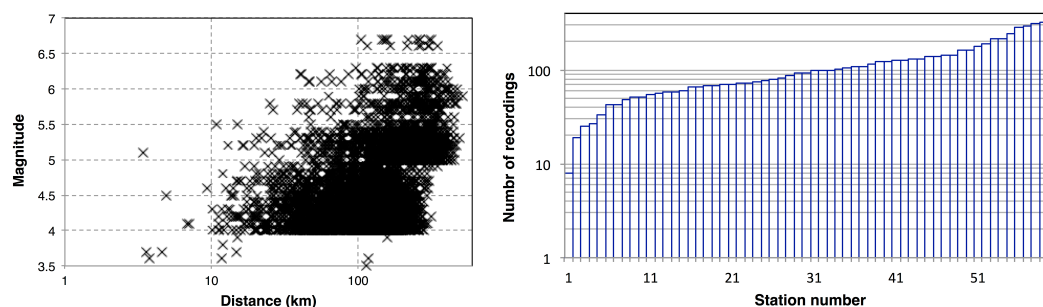


Figure 2: a. Indicative distribution of magnitude (local) and distance (epicentral) for all data analysed in this study. Station-specific plots can be found in the Supplement (Figs S1 and S2). b. Number of recordings used per station.



110 2.2 Creation of a new strong-motion dataset

The data we select come from the period 2012–2021, depending on when each station began to operate in real-time, its period of operation and data availability. We use the catalogue of NOA (<https://eida.gein.noa.gr/fdsnws/availability/1>) and search for recordings following the criteria mentioned above. We retrieve raw waveforms and station xml from EIDA@NOA and apply instrument correction to retrieve physical units. We check raw HH data for clipping and discard all such instances. We use an in-house software that follows closely upon the rationale described in Kishida et al. (2016), the procedure that underpins the NGA-East processing (Goulet et al., 2014). We first perform visual inspection in the time domain (Fig. 3a), where the windowing has been automatically done based on the origin time (P and S arrivals, selection of equal duration pre-event noise and signal windows). The signal window includes all wave packages of engineering interest, i.e. all S waves and the most energetic surface waves. All automatic picks are assessed and corrected as necessary. We then perform visual inspection in the frequency domain (Fig. 3a), assessing smoothed and unsmoothed S-wave and noise Fourier amplitude spectra (FAS) of acceleration. Aside from the signal-to-noise ratio (SNR=3 threshold), we also consider the fit to the omega-square source model (Brune 1970; 1971). Figure 3 shows an example of window selection in the time domain, and of the lowest and highest usable frequencies (LUF, HUF) in log and linear scale respectively. All FAS will be used within their usable frequency to compute the empirical transfer functions in what follows.

125

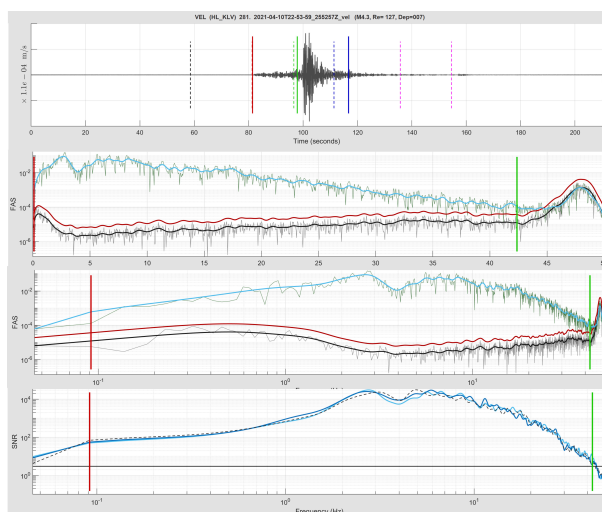


Figure 3: Top to bottom: Example manual processing: windowing of a velocity trace in the time domain, selecting the HUF and LUF in the frequency domain (in linear and log scale respectively) for the two horizontal acceleration FAS, and inspection of the SNR.



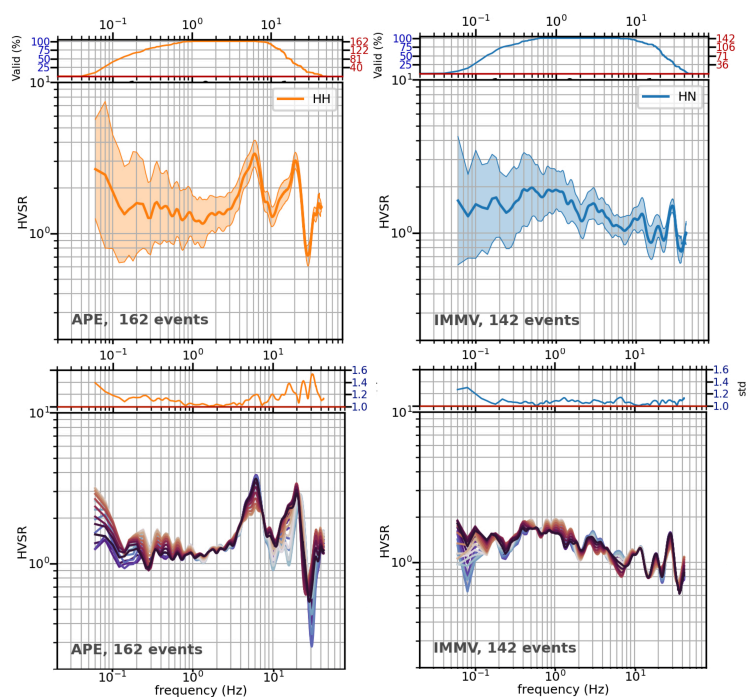
130

2.3 Transfer functions

The start of the S-wave windows is taken early enough so as for the first S waves not to be affected by the tapering. The acceleration FAS are computed and smoothed with a Konno & Ohmachi (1998) $b=40$ mild smoothing. We compute the horizontal-to-vertical spectral ratio (HVSr; Lermo & Chavez-Garcia, 1993) for each component of each recording at each station. The mean HVSr per site is computed as the log average across all events, as is customary, and as Ktenidou et al. (2011) showed that spectral ratio ordinates are lognormally distributed. At each frequency, the mean is computed out of the available recordings within the legitimate bandwidth. Within the range of 1-10 Hz, typically all recordings are usable, which as noise increases towards lower and higher frequencies, fewer recordings are strong enough to contribute. The two components of each FAS are combined as the square root of the sum of squares (SRSS) so as to yield an orientation-independent estimate. Fig. 4 (top) shows two examples of this mean HVSr ± 1 SD. We note that the curves are only drawn where the number of usable events is at least 5, in order to ensure a more robust estimate of the statistics (most ground motion applications will accept a minimum of 3). Figures S4 and S5 in the Supplement show results for all HH and HN stations respectively.

135

140



145

Figure 4: Example HVSR results for stations APE.HH (left) and IMMV.HN (right). Top row: mean, direction-invariant (SRSS) HVSR ± 1 standard deviation; inset on top indicates the number and percentage of usable recordings per frequency. Bottom row: HVSR per component, as those are rotated by 10-degree intervals from North to East; inset on top indicates the standard deviation (hence, directional sensitivity or variability) per frequency.

150

A reference site is expected to exhibit a HVSR that is relatively flat and close to unity. Departure from reference site conditions has been judged in different ways across different studies. A few example thresholds include the typical value of HVSR >2 , but also HVSR $>2\sqrt{2}$ (Lanzano et al., 2020 from Puglia et al., 2011), and the more generous one of HVSR >3 (Pilz et al., 2020). Of course, HVSR is an approximation, and generally an underestimation with respect to the ‘true’ site transfer function, for instance as that may be computed using the standard spectral ratio (SSR) of Borchardt (1970), i.e., using an actual rock recording as reference rather than the vertical. The assumed premise of HVSR should not be that the vertical component actually remains unaltered by stratigraphy (or, indeed, by other geomorphological features), but rather than it is expected to exhibit amplification at frequencies higher than the ones the horizontal ground motion amplifies around, thus permitting a rather clear identification of at least the first resonant peak, albeit at a generally lower level than the actual. It is

155



160 for this reason that we take the stricter view of a threshold of $HVSR > 2$ when attempting to identify potential reference sites
among our group of 60 stations.

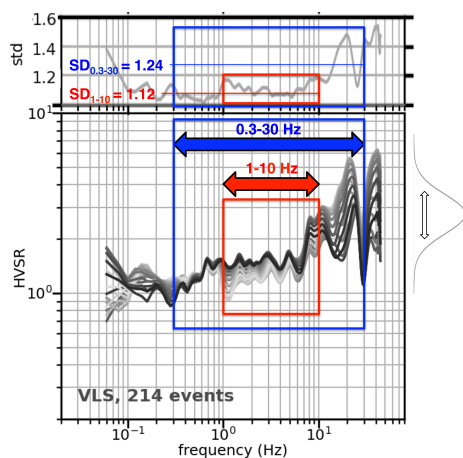
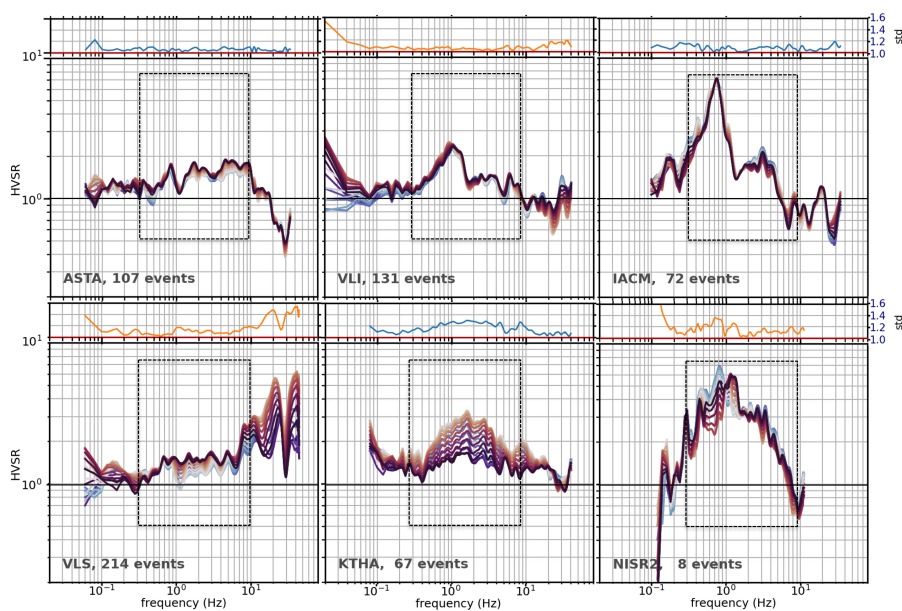


Figure 5: Illustration of the two frequency bands over which the standard deviation from the rotations is averaged, to derive
165 an index of directional variability: 0.3-30 Hz (blue) and 1-10 Hz (red). For station VLS, the value is low for the narrow band
(1.12) but high for the wider one (1.24) due to high-frequency variability.

We also expect a reference site to not exhibit strong directional dependence, i.e., reference ground motions not to be
sensitive to the sensor installation orientation. However, checking only the difference between the two horizontal
170 components as installed is not rigorous enough. The sensors are installed in the N and E directions, which are arbitrary with
respect to each site's potential geomorphological features. This is why we follow the technique of Ktenidou et al. (2016) to
assess the variability of site response to azimuth. We rotate each time series by successive increments of 10° , from 0° - 90° ,
and recompute the FAS and HVSR each time, so as to discover whether there are any other directions that may bring out
directional differences. Such differences we view as an indication of departure from 1D behaviour due to local
175 geomorphology (basin edges, topography, lateral discontinuities, etc.). All of these factors can cause amplification of
different levels in the two horizontal components, e.g. the radial and transverse with respect to the feature's axis. Fig. 4
(bottom) shows two examples of the mean HVSR per component, as the as-installed motions are rotated by 10-degree
increments from North to East. The inset on top indicates the standard deviation of the mean HVSR values across all rotations
per frequency. We consider this as an index of the directional variability of each station's site response. Though the typical
180 parameters extracted from such calculations are most of all the resonant frequency f_0 , and –to some extent of credibility,
mostly as an indication- the corresponding amplitude A_0 and perhaps the same metrics for the first higher mode, if



applicable, we also take note of the directional variability of the transfer function amplitude. To this end, we compute the mean of this variability function with frequency across two indicative ranges of interest, namely a wide one spanning 2 orders of magnitude (0.3-30 Hz) and a narrower one of 1 order of magnitude, which may also be more interesting for typical structural response (1-10 Hz). We also note the value of this function around the resonant frequency of the site. We propose that these three values ($SD_{0.3-30}$, SD_{1-10} , SD_{f_0}) can be used as approximate indicators of the azimuthal stability of site response. Figure 5 illustrates these values for station VLS, where such scatter begins above 10 Hz and thus affects mostly $SD_{0.3-30}$ (1.24) and SD_{f_0} (1.48 at 20 Hz). The value of SD_{1-10} (1.12) is relatively low for this dataset. In the examples of Fig. 4, station APE exhibits non-negligible directional variability around its f_0 of 6.1 Hz, so it is a rather poor reference site candidate, with not only a clear amplification peak reaching above 3 based on 162 recordings (top plot), but also exhibits directional sensitivity of 1.20 (bottom plot). In contrast, station IMMV appears to be a very good candidate, lacking any identifiable peak and having sensitivity around 1.07.



195 **Figure 6:** Indicative examples of HVSR: From left to right: low, medium and high amplification within the range of 0.3-10 Hz. From top to bottom, lower and higher variability with azimuth.

Figure 6 illustrates a few characteristic examples. Considered in the band 0.3-10 Hz, ASTA is the best reference candidate with no amplification and very low SD, followed by VLS, with rather higher variability (yet still a rather acceptable



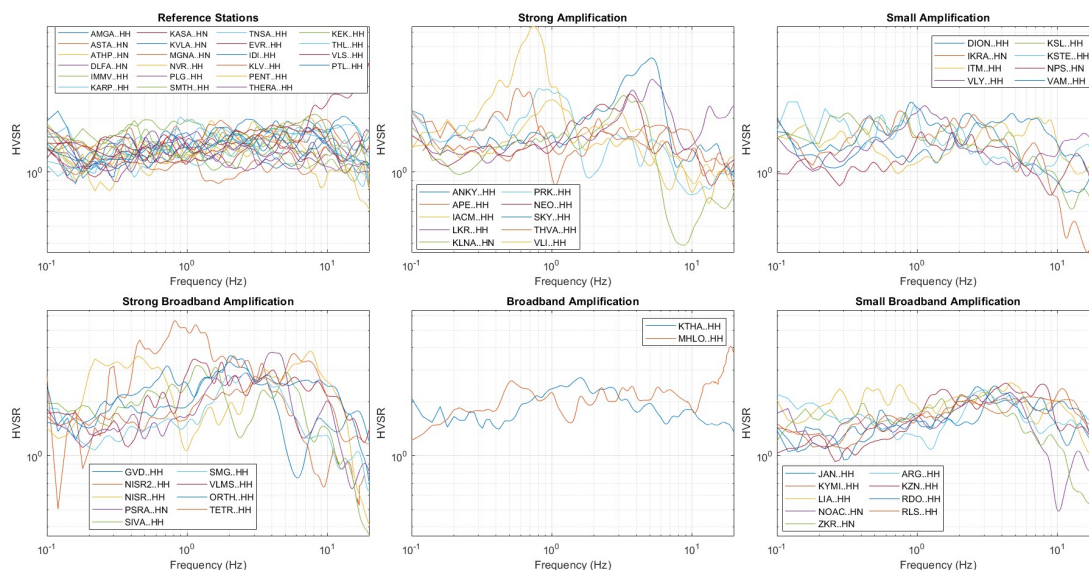
200 reference below 10 Hz). VLI exhibits a weak but clear low-frequency resonance, while IACM a clear and very strong one,
with also a rather clear first higher mode. None of these two show directional variability. KTHA and NISR2, on the other
hand, show weak and strong peaks respectively which are rather broadband (not so 'peaky' as their counterparts VLI and
IACM), and in addition possess a very high degree of directionality. The behaviour of most of these stations is certainly not
205 what we would expect of 'rock stations'. Based on such geological 'labels', one might be typically consider them as reliable
reference stations, assuming no great amplification. Nonetheless, we see cases of either low or high-frequency (VLS)
amplifications up to 6-8. In addition to that, for $SD > 1.20$, what one would perceive as the 'reference' ground motion would
depend very much on the orientation in which the sensor happened to be placed, since we see differences of up to factors of
2 or even 3 at certain frequencies. Figures S6 and S7 in the Supplement show results for all HH and HN stations
respectively.

210 Based on such observations, we can group the stations of this study into a few indicative categories. We name these:
reference station, small/large amplification, and small/large broadband amplification. Other groupings could be envisioned,
but our goal here is to call attention to the main behaviours and how they deviate from the expected (flat) rock response.
Figure 7 shows these groups. We do not investigate on a station-by-station basis what exactly lies behind the amplification
patterns we observe. Considering these are generally thought to be rock sites, we only mention a few possible interpretations
215 (other than geological misclassification). It is known that sharp high-frequency peaks can be due to shallow soft or
weathered layers on bedrock, and their level will increase with the impedance (V_s) contrast between the two materials. A
directional dependence of such a peak could signify 2D or 3D effects stemming from non-horizontal conditions. A low-
frequency, relatively low peak could indicate a deep interface, likely between soft and harder rock. Given the hardness of the
sites, another likely physical mechanism is topographic amplification, which would be expected to take place at specific
220 frequencies, depending on the overall material V_s and the height/width of the hill/slope/topographic feature (Geli et al.,
1988; Ashford & Sitar, 1997). In this case, the spectral peak will also exhibit directionality, since such amplification is
known to be strongest in a certain direction, such as transversely to the axis of a 2D ridge. We expect the interpretation to be
more complex in the case of a 3D feature such as a hill or cave (instances of which exist in our database, see next section).

In Table 2 we compile some basic metadata for the 60 stations (such as N_{rec} , M range), along with the results of the
225 assessment presented in this section, namely: f_0 , A_0 , f_1 , S1 (if applicable), $SD_{0.3-30}$, SD_{1-10} , SD_{f_0} , and description of
amplification. We also include an additional calculation: the maximum amplitude that the transfer function reaches if we
correct the HVSR for the implicit amplification of the vertical component. To do so, we use the function proposed by Ito et
al. (2020) called VACF (correction function for vertical amplification). This has its limitations, since VACF was calibrated
on Japanese data, but we consider it a not illogical first approximation, coming from a region of similar (active) tectonic
230 regime. VACF has been constrained within a narrower band than used in this study, namely from 0.12-15 Hz. An example is
shown in the Supplement (Fig. S3). Table 2 includes field A_{0_corr} in an indicative role, as a rough indication of the potential
absolute amplification at the sites, and not to be used at face value for hazard or other calculations.



We note that any very strongly nonlinear recordings (though this is not very probable for rock/stiff conditions) would be eliminated at the visual inspection stage, while weaker ones may still remain, since we assume they would not bias the ensemble mean results enough to merit a dedicated check. If present, we expect nonlinearity to decrease the level of high-frequency peaks. Since we are rather strict in our use of a threshold of 2 rather than 2.8 or 3, we believe it is not a grave issue.



240 **Figure 7:** Groups of stations with similar amplification.

3 Compiling other station metadata

3.1 Rationale

There have been studies and projects dedicated to assessing the most useful parameters and proxies in describing site conditions.

a. Cultrera et al. (2021) conducted a wide European survey including various end users and considering aspects such as cost and difficulty in procuring the parameters, which concluded that the preferred 7 indicators out of a total of 24 –some being admittedly not very common– are the following: 1. fundamental frequency f_0 ; 2. full Vs profile; 3. V_{S30} ; 4. depth to seismological bedrock; 5. depth to engineering bedrock; 6. surface geology; and 7. soil class. We note that some of these are direct derivatives of others (3 hinging upon 2 and 7 depending on 2 and 4).



b. Lanzano et al. (2020) conducted a study in Central Italy focusing on rock sites in particular, and proposed an algorithm that takes into account 6 site descriptors, grading and combining them mathematically to produce an overall qualifier for characterising reference stations. Their proxies used to identify rock stations are: 1. housing/installation conditions; 2. topographic conditions; 3. surface geology (same as 6 above); 4. V_{S30} (same as 3 above); 5. shape of HVSr from noise or earthquakes (related to 1 above); 6. δs_2s , the site-to-site term resulting from GMPE residuals analysis using response spectra, as an alternative estimate of the transfer function.

c. Pilz et al. (2020) assess reference stations at a European level from homogenized data considering the following parameters: 1. surface geology (as above); 2. slope/topography (as above); 3. HVSr (as above); 4. similarity of surface κ_0 (high-frequency site attenuation) to coda κ_0 , which is considered as indicative of deeper conditions; 5. ML station residuals.

260 In the previous section we computed FAS-based HVSr for the first time for these stations, and in this section we compile all existing parameters we can find from various sources: housing/installation, topography/slope, surface geology, and V_{S30} (ad-hoc V_s profiles being almost non-existent in Greek seismic rock stations). To this literature-based collation, we also add insights based on site visits by NOA personnel. We believe this is important because geological maps constructed for an entire country inevitably contain errors and simplifications, whereas a site walkover of the station location by an experienced geologist provides additional reliability. Similarly, satellite-based estimates of slope/topography invariably include approximation, homogenisation and some lack of specificity depending on the size of the ‘pixel’, whereas again a site visit laves little doubt as to the exact nature of the landscape at the station.

3.2 Station installation

Table 3 compiles the information we found on housing and installation conditions at our 60 rock stations. Information for the HN stations is available from the website <https://accelnet.gein.noa.gr/station-information/> (last accessed: December 2023), while additional detail specially for the HH stations is provided based on site visits, with more detailed descriptions given in the dedicated article on EIDA@NOA (Evangelidis et al., 2021). The last column of the table provides our assessment as to whether each station can be considered a reference station based on installation conditions. We note here that housing condition for HL network are vastly different to those of other countries, with explicit free-field conditions being rather rare. 275 The Italian equivalent (Lanzano et al., 2020) only makes reference to two types of stations, free-field and in power towers, while the NOA network has had to make use of environments as diverse as monastery cells. However, in all cases where a ‘vault’ is mentioned, this is created within the structure hosting it by cutting around the station in a way so as to isolate its potential motion from that of the surrounding structure, hence avoiding soil-structure interaction effects.

3.3 Topography and slope

280 Table 4 compiles the information gathered on terrain slope and topographic conditions at our stations. There are various sources. For the HN stations, ESM (<https://esm-db.eu/>; Lanzano et al., 2021; Luzi et al., 2016) provide the slope in degrees along with their classification into four categories with the following code: T1: ‘Flat surface, isolated slopes and cliffs with



average slope angle $i \leq 15^\circ$; T2: 'Slopes with average slope angle $i > 15^\circ$ '; T3: 'Ridges with crest width significantly less than the base width and average slope angle $15^\circ \leq i \leq 30^\circ$ '; T4: 'Ridges with crest width significantly less than the base width and average slope angle $i > 30^\circ$ '. For the HN stations again, Margaris et al. (2021) provide an estimate of slope which we have also converted into degrees and which for the most part almost coincides with the angles by ESM (save 2 stations marked in the table in bold italics, DLFA and NOAC, where however the difference does not cause a change in ESM code). For the entirety of stations studied here, additional detail is also provided based on site visits, where we group stations into the following categories: 1. Flat/shallow (< 15) within 200 m; 2. Steep (< 30) within 200 m; 3. Steep hill crest; 4. Near cliff. This offers new information for about 35 stations for which no information was available before, some of them on various kinds of steep conditions.

3.4 V_{s30}

Table 5 compiles the information gathered on V_s at our study's rock stations. There are again various sources. For the HN stations, ESM again provides the proxy-based V_{s30} using slope (and consequent EC8 soil class as per CEN, 2004), while Margaris et al. (2021) provide a variety of estimates of V_{s30} . A couple come from measurements in the vicinity of the stations (within 1 km, as per Stewart et al., 2014), while most are derived from proxies, using not only ground slope but also terrain, and a single value per station is given as preferred by that study. We note that although Stewart et al. (2014) was based on entire V_s profiles, that study did not release any profiles as functions of depth, but rather their derived average V_{sz} values over a given depth z . Finally, a couple of stations have been characterised ad hoc at the station location by NOA within the national project HELPOS (Deliverable 2.5.3, Geophysical measurements at seismic stations). Between the three sources of information, namely ESM, Margaris et al. (2021) and HELPOS, there are in some cases discrepancies. The strongest contradictions that correspond to, say, a factor of 2-3 of difference in V_{s30} and a clear jump in site class, are marked in Table 5 in bold italics, such as ATHP, IACM, KASA, KSL, SMTH. In the case of measured V_s profiles on the spot (HELPOS), we consider those as the definitive V_{s30} estimates. However, in the case of measurement within 1 km distance from the station, we believe their validity very much depends on lateral variations in stratigraphy and so do not attach more confidence to them than the proxy-based ones of ESM.

3.5 Geology

Table 6 compiles all the information gathered on surface geology at our study's rock stations. Information for the HN stations is available from the website <https://accelnet.gein.noa.gr/station-information/> (last accessed: December 2023). Description of the geological unit and age are provided for HN stations by Margaris et al. (2021). Finally, 17 of our 60 stations were also found in the list of Pilz et al. (2020) for European reference sites, and in those cases we also report the unified geological descriptors attributed by them according to the European Geological Data Infrastructure (EGDI). Two of those attributes were based on AI and are noted as such in the table.



One of the important features of this study is that we provide new information for the entirety of stations, consisting of
 315 geological unit and age descriptions. This is based on the combination of site visit and walkover experience with the detailed
 revisiting of maps and literature. The majority of stations were located in 53 geological maps (1:50,000 scale) published by
 the Hellenic Survey of Geology and Mineral Exploration (HSGME) and their geology interpreted in conjunction with
 knowledge of the local features from sit visits. Geological conditions for a couple of stations were derived from relevant
 publications indicated in Table 6 with an asterisk. There are several contradictions between the various sources, too
 320 numerous to discuss in detail here. Our best estimate after assessing all available information and experience is given in the
 relevant columns ‘this study’.

Table 1. General information and metadata for the stations in this study and statistics on the ground-motion data analysed.

325

N o.	Station code	Cha nne l	Station Name	Network code	StLat (deg)	StLon (deg)	StEl (m)	Period	ML range	Nrec
1	AMGA	HNc	AMORGOS	HL	36.83156	25.89384	308	2012-2019	4-6.2	60
2	ANKY	HNc	ANTIKYTHIRA	HL	35.86704	23.30117	143	2012-2021	4-6.6	110
3	APE	HH	APEIRANTHOS, NAXOS	HL/GE	37.07274	25.52301	608	2012-2021	4-6.3	162
4	ARG	HH	ARCHANGELOS, RHODES	HL	36.21356	28.12122	148	2012-2021	4-6.7	124
5	ASTA	HN	ASTYPALAI	HL	36.54552	26.35295	64	2012-2020	4-6.7	129
6	ATHP	HN	ATHENS-NEO PSYCHIKO	HL	38.00080	23.77349	187	2020-2021	4-6.0	25
7	DION	HNc	DIONYSOS ATTIKIS	HL	38.07794	23.93306	460	2013-2016	4-6.3	33
8	DLFA	HN	DELFOI	HL	38.47836	22.49583	570	2012-2021	4-6.6	316
9	EVR	HH	EVRTANIA	HT	38.91657	21.81050	1037	2012-2021	4-6.1	296
10	GVD	HNc	GAVDOS	HL	34.83914	24.08738	170	2012-2017	4-6.2	86
11	IACM	HNc	HERAKLEIO	HL	35.30580	25.07090	45	2017-2021	4-6.3	72
12	IDI	HH	ANOGEIA	HL/MN	35.28878	24.89043	750	2012-2021	4-5.5	161
13	IKRA	HN	AGIOS KIRIKOS IKARIA	HL	37.61117	26.29283	30	2012-2017	4-6.3	79
14	IMMV	HNc	CHANIA, CRETE	HL/GE	35.46060	23.98110	230	2012-2021	4-6.2	142
15	ITM	HNc	ITHOMI MESSINIA	HL	37.17872	21.92522	423	2018-2017	4-6.0	217
16	JAN	HNc	IOANNINA	HL	39.65616	20.84874	526	2012-2022	4-6.6	177
17	KARP	HNc	KARPATHOS	HL	35.54710	27.16106	524	2012-2021	4-6.7	284
18	KASA	HN	KASSIOPI	HL	39.74628	19.93542	65	2012-2018	4-6.0	73
19	KEK	HH	KERKYRA	HL/MN	39.71270	19.79623	227	2012-2022	4-6.6	98
20	KLNA	HN	KALYMNOS	HL	36.95708	26.97274	28	2013-2021	4-6.7	240
21	KLV	HH	KALAVRITA	HL	38.04350	22.15040	758	2012-2021	4-6.6	322
22	KSL	HNc	KASTELLORIZO	HL	36.15031	29.58561	64	2012-2021	4-6.7	77
23	KSTE	HNc	KASTELLI, CRETE	HL	35.18010	25.33720	395	2021-2021	3.5-5.7	19
24	KTHA	HNc	KYTHIRA	HL	36.25660	23.06210	360	2013-2021	4-6.2	67
25	KVLA	HN	KAVALA	HL	40.93704	24.38591	122	2012-2022	4-6.1	52
26	KYMI	HNc	KYMI	HL	38.63315	24.10014	259	2014-2021	4-6.7	99
27	KZN	HH	KOZANI	HL	40.30331	21.78209	791	2012-2021	4-5.9	121
28	LIA	HNc	LIMNOS	HL	39.89725	25.18055	67	2012-2022	4-6.7	107
29	LKR	HH	ATALANTI LOKRIDA	HL	38.64957	22.99881	192	2012-2017	4-6.3	94
30	MGNA	HN	MEGANISSI LEUKADA	HL	38.65606	20.79116	58	2012-2014	4-5.8	75
31	MHLO	HH	PLAKA, MILOS ISLAND	HL	36.68984	24.40171	175	2012-2021	4-6.3	190
32	NEO	HH	NEOCHORI VOLOS	HL/MN	39.30567	23.22189	510	2012-2022	4-6.3	141
33	NISR	HNc	NISYROS ISLAND	HL	36.61060	27.13090	44	2021-2021	4-6.7	94
34	NISR2	HH	VOLCANOGOLY MUSEUM, NISYROS	HL	36.57441	27.17666	423	2021-2021	4-5.7	8
35	NOAC	HNc	ATHENS- THISSEIO	HL	37.97384	23.71767	93	2012-2018	4-6.3	128
36	NPS	HH	NEAPOLIS CRETE	HL	35.26134	25.61037	288	2012-2016	4-6.2	58
37	NVR	HNc	KATO NEVROKOPI	HL	41.34846	23.86517	627	2012-2021	4-6.3	48
38	ORTH	HH	ORTHONIES, ZAKYNTHOS	HL	37.85112	20.69627	450	2018-2020	4-5.9	65
39	PENT	HH	PENTALOFOS KOZANIS	HL	40.19588	21.13842	1096	2012-2021	4-6.0	55
40	PLG	HNc	POLIGIROS CHALKIDIKI	HL	40.37328	23.44443	566	2013-2013	4-6.3	42
41	PRK	HNc	AGIA PARASKEVI LESVOS	HL	39.24565	26.26499	130	2013-2022	4-6.7	100



42	PSRA	HN	PSARA	HL	38.53978	25.56202	13	2012-2018	4-6.3	71
43	PTL	HH	PENTELI	HL	38.04730	23.86380	500	2012-2021	4-6.6	142
44	RDO	HH	RODOPI	HL	41.14503	25.53553	116	2012-2020	4-6.1	58
45	RLS	HH	RIOLOS KATO ACHAEA	HL	38.05586	21.46475	97	2012-2021	4-6.6	328
46	SIVA	HNc	SIVAS CRETE	HL/GE	35.01777	24.81204	96	2012-2021	4-6.3	42
47	SKY	HH	SKYROS	HL	38.88310	24.54820	268	2012-2022	4-6.3	70
48	SMG	HNc	SAMOS	HL	37.70425	26.83772	348	2020-2022	4-6.3	51
49	SMTH	HNc	SAMOTHRAKI	HL	40.47094	25.53045	365	2012-2022	4-6.7	68
50	TETR	HH	TETRAKOMO	HL	39.34450	21.27467	942	2018-2022	4-5.9	66
51	THERA	HH	ANCIENT THERA, SANTORINI	HL/GE	36.36699	25.47526	288	2019-2021	4-6.3	83
52	THL	HH	KLOKOTOS	HL/MN	39.56468	22.01440	86	2012-2022	4-5.4	116
53	THVA	HH	IEK THIVAS	HL	38.32983	23.33601	214	2020-2021	4-5.9	27
54	TNSA	HN	TINOS	HL	37.53942	25.16310	21	2012-2021	4-6.7	125
55	VAM	HH	VAMOS	HL	35.40700	24.19970	225	2012-2021	4-6.3	139
56	VLI	HH	VELIES LAKONIA	HL	36.71803	22.94686	220	2012-2021	4-6.2	131
57	VLMS	HNc	VOLIMES- ZAKYNTHOS	HL	37.87670	20.66293	431	2014-2015	4-5.8	56
58	VLS	HH	VALSAMATA KEFALONIA	HL	38.17683	20.58860	402	2012-2021	4-5.9	214
59	VLY	HH	BOYLA ATTIKHS	HL	37.85240	23.79420	256	2012-2022	4-6.3	103
60	ZKR	HNc	ZAKROS	HL/GE	35.11470	26.21691	254	2012-2019	4-6.2	106

Table 2. Detailed results of the HVSR analysis for the stations in this study.

No.	Station code	f_0 (Hz)	A_0	f_1 (Hz)	A_1	A_{0_corr}	$SD_{0.3-30}$	SD_{1-10}	SD_{10}	Amplification group	Potential reference site?
1	AMGA	-	-	-	-	-	1.05	1.04	-	Reference station	yes
2	ANKY	0.8	2.75	-	-	5	1.11	1.06	1.36	Strong LF amplification	no
3	APE	6.2	3.4	20	3	7	1.19	1.09	1.20	Strong HF amplification	no
4	ARG	3	2.3	-	-	5	1.18	1.13	1.21	Small broadband amplification	ok
5	ASTA	-	-	-	-	-	1.05	1.07	-	Reference station	yes
6	ATHP	-	-	-	-	-	1.12	1.1	-	Reference station	yes
7	DION	2.3	2.1	-	-	4.2	1.13	1.13	1.09	Small amplification	ok
8	DLFA	-	-	-	-	-	1.07	1.05	-	Reference station	yes
9	EVR	-	-	-	-	-	1.13	1.07	-	Reference station	yes
10	GVD	0.3	2.1	2	3.3	5.5	1.06	1.05	1.06	Broadband strong amplification	no
11	IACM	0.75	6.5	3.1	2.1	11	1.08	1.07	1.05	Very strong LF amplification	no
12	IDI	-	-	-	-	-	1.06	1.09	-	Reference station	yes
13	IKRA	0.4	2.1	0.75	2.3	1.9	1.1	1.07	1.09	Small amplification	ok
14	IMMV	-	-	-	-	-	1.06	1.07	-	Reference station	yes
15	ITM	-	-	-	-	-	1.11	1.09	-	Small HF amplification	ok
16	JAN	-	-	-	-	4.1	1.1	1.07	1.02	Small broadband amplification	ok
17	KARP	-	-	-	-	3.9	1.11	1.04	1.05	Reference station	yes
18	KASA	-	-	-	-	-	1.07	1.07	-	Reference station	yes
19	KEK	-	-	-	-	5	1.17	1.17	1.23	Small HF amplification	ok
20	KLNA	3.2	2.7	-	-	-	1.09	1.11	1.19	Strong amplification	no
21	KLV	-	-	-	-	-	1.06	1.06	-	Reference Station	yes
22	KSL	-	-	-	-	-	1.09	1.17	-	Small LF amplification	ok
23	KSTE	-	-	-	-	4.7	1.13	1.13	1.06	Small LF amplification	ok
24	KTHA	1.6	2.7	-	-	3.6	1.11	1.2	1.30	Broadband amplification	no
25	KVLA	-	-	-	-	-	1.07	1.04	-	Reference Station	yes
26	KYMI	11	2.4	-	-	4.8	1.16	1.13	1.25	Small broadband amplification	ok
27	KZN	1.5	2.3	4.5	2.5	3.7	1.13	1.14	1.15	Small broadband amplification	ok
28	LIA	25	3.2	-	-	5.1	1.11	1.1	1.11	Small broadband amplification	ok
29	LKR	3.8	2.9	5.2	3.3	7.1	1.23	1.13	1.14	Strong Amplification	no
30	MGNA	-	-	-	-	-	1.1	1.09	-	Reference Station	yes
31	MHLO	0.5	2.6	-	-	3.1	1.1	1.07	1.11	Broadband amplification	no
32	NEO	3.6	2.7	-	-	5	1.14	1.13	1.11	Strong amplification	no
33	NISR	7.7	3.8	-	-	8.5	1.14	1.2	1.09	Broadband strong amplification	no
34	NISR2	0.8	5.6	-	-	10	1.15	1.12	1.33	Broadband strong amplification	no
35	NOAC	-	-	-	-	-	1.11	1.14	-	Small broadband amplification	ok
36	NPS	-	-	-	-	4.1	1.1	1.09	1.12	Reference Station	yes
37	NVR	7.3	2	-	-	4	1.09	1.05	1.05	Small HF amplification	ok
38	ORTH	0.7	3.2	2	3.6	4.3	1.07	1.1	1.10	Broadband strong amplification	no
39	PENT	-	-	-	-	-	1.13	1.08	-	Reference Station	yes
40	PLG	-	-	-	-	-	1.09	1.04	-	Reference Station	yes
41	PRK	1.1	2.9	-	-	6	1.1	1.07	1.06	Strong LF amplification	no
42	PSRA	4	3.8	-	-	8.5	1.05	1.06	1.03	Broadband strong amplification	no



43	PTL	-	-	-	-	1.07	1.08		Reference Station	yes	
44	RDO	3.5	2.4	27	2.6	3.6	1.13	1.06	1.07	Small broadband amplification	ok
45	RLS	-	-	-	-	-	1.14	1.06		Small broadband amplification	ok
46	SIVA	1.2	3.2	5	2.9	5.8	1.12	1.08	1.04	Broadband strong amplification	no
47	SKY	5.2	4.3	-	-	10	1.11	1.07	1.15	Very strong amplification	no
48	SMG	2	2.8	2.7	2.9	5	1.15	1.09	1.13	Broadband strong amplification	no
49	SMTH	-	-	-	-	-	1.05	1.09		Reference station	yes
50	TETR	5.7	3.7	-	-	7.3	1.18	1.13	1.09	Broadband strong amplification	no
51	THERA	-	-	-	-	-	1.23	1.21		Reference Station	yes
52	THL	-	-	-	-	-	1.05	1.06		Reference Station	yes
53	THVA	0.6	2.9	-	-	3.7	1.15	1.14	1.12	Strong amplification	no
54	TNSA	-	-	-	-	-	1.08	1.12		Reference station	yes
55	VAM	0.45	2.1	0.9	2.45	2.1	1.12	1.17	1.21	Small amplification	ok
56	VLI	1	2.52	-	-	5	1.09	1.06	1.04	Strong amplification	no
57	VLMS	1.1	3.5	1.8	3.3	7	1.13	1.11	1.24	Broadband strong amplification	no
58	VLS	21	4.4	-	-	-	1.24	1.12	1.45	Reference station	yes
59	VLY	1.1	2.3	-	-	4.4	1.08	1.1	1.05	Small amplification	ok
60	ZKR	3.1	2.2	5	-	-	1.12	1.09	1.09	Small broadband amplification	no

330

Table 3. Housing and installation conditions for the stations in this study.

No.	Station code	StEI (m)	Building type (from accelnet)	Installation condition - site visit	Potential reference site?
1	AMGA	308	1-floor RC	not free field	no
2	ANKY	143	-	free field only for HH	no
3	APE	608	-	vault in building	yes
4	ARG	148	-	vault in building	yes
5	ASTA	64	2-floor adobe masonry	not free field	no
6	ATHP	187	3-floor RC	not free field	no
7	DION	460	-	cave	no
8	DLFA	570	3-floor RC	not free field	no
9	EVR	1037	-	vault in building	yes
10	GVD	170	-	free field	yes
11	IACM	45	-	free field	yes
12	IDI	750	-	underground vault	yes
13	IKRA	30	2-floor RC	not free field	no
14	IMMV	230	-	monastery cell on rock	no
15	ITM	423	-	vault in building	yes
16	JAN	526	1-floor RC	vault in building	yes
17	KARP	524	-	vault in small building	yes
18	KASA	65	2-floor RC	not free field	no
19	KEK	227	-	vault in small building	yes
20	KLNA	28	3-floor RC	not free field	no
21	KLV	758	-	digged cave	no
22	KSL	64	-	vault in small building	yes
23	KSTE	395	-	vault in small building	yes
24	KTHA	360	-	monastery cell on rock	no
25	KVLA	122	2-floor RC	not free field	no
26	KYMI	259	1-floor RC	vault in small building	yes
27	KZN	791	1-floor RC	vault in building	yes
28	LIA	67	1-st RC	free field only for HH	no
29	LKR	192	1-floor RC	vault in building	yes
30	MGNA	58	2-floor RC	not free field	no
31	MHLO	175	-	not free field	no
32	NEO	510	-	vault in building	yes
33	NISR	44	-	not free field	no
34	NISR2	423	-	free field	yes
35	NOAC	93	-	vault in building	yes
36	NPS	288	-	vault in building	yes
37	NVR	627	1-floor RC	free field	yes
38	ORTH	450	-	not free field	no
39	PENT	1096	-	not free field	no
40	PLG	566	1-floor RC	vault in building	yes



41	PRK	130	1-floor RC	vault in building	yes
42	PSRA	13	2-floor RC	not free field	no
43	PTL	500	-	vault in building	yes
44	RDO	116	-	vault in small building	yes
45	RLS	97	-	vault in building	yes
46	SIVA	96	1-floor masonry	free field	yes
47	SKY	288	-	not free field	no
48	SMG	348	-	vault in small building	yes
49	SMTH	365	1-floor RC	underground vault	yes
50	TETR	942	-	vault in small building	yes
51	THERA	288	-	free field	yes
52	THL	86	1-floor RC	dug vault in rock	yes
53	THVA	214	1-floor RC	not free field	no
54	TNSA	21	2-floor RC	not free field	no
55	VAM	225	-	vault in building	yes
56	VLI	220	-	vault in small building	yes
57	VLMS	431	free-field	free field	yes
58	VLS	402	-	vault in building	yes
59	VLY	256	-	free field	yes
60	ZKR	254	1-floor RC	not free field	no

335 **Table 4.** Topography and slope conditions for the stations in this study.

No.	Station code	StEI (m)	Topography code (ESM)	Slope angle° (ESM)	Slope (Marg2021)	Slope angle° based on Marg2021	Topography assessment by site visits	Potential reference site?
1	AMGA	308	T1	3	0.047	3	Flat/shallow (<15) within 200 m	yes
2	ANKY	143	T1	8	0.138	8	Flat/shallow (<15) within 200 m	yes
3	APE	608	-	-	-	-	Flat/shallow (<15) within 200 m	yes
4	ARG	148	T1	-	-	-	Flat/shallow (<15) within 200 m	yes
5	ASTA	64	T1	9	0.14	8	Flat/shallow (<15) within 200 m	yes
6	ATHP	187	T1	2	-	-	Flat/shallow (<15) within 200 m	yes
7	DION	460	T3	2	-	-	Flat/shallow (<15) within 200 m	yes
8	DLFA	570	T4	38	0.502	27	Steep (<30) within 200 m	no
9	EVR	1037	-	-	-	-	Flat/shallow (<15) within 200 m	yes
10	GVD	170	T1	2	0.035	2	Flat/shallow (<15) within 200 m	yes
11	IACM	45	T1	11	-	-	Flat/shallow (<15) within 200 m	yes
12	IDI	750	-	-	-	-	Steep (<30) within 200 m	no
13	IKRA	30	-	-	0.129	7	Flat/shallow (<15) within 200 m	yes
14	IMMV	230	T2	18	-	-	Flat/shallow (<15) within 200 m	yes
15	ITM	423	T1	13	0.223	13	Flat/shallow (<15) within 200 m	yes
16	JAN	526	T1	2	0.056	3	Flat/shallow (<15) within 200 m	yes
17	KARP	524	T3	11	-	-	Steep hill crest	no
18	KASA	65	T4	17	0.321	18	Steep (<30) within 200 m	no
19	KEK	227	-	-	-	-	Steep (<30) within 200 m	no
20	KLNA	28	T1	4	0.065	4	Flat/shallow (<15) within 200 m	yes
21	KLK	758	-	-	-	-	Steep (<30) within 200 m	no
22	KSL	64	T3	9	0	0	Steep hill crest	no
23	KSTE	395	-	-	-	-	Steep (<30) within 200 m	no
24	KTHA	360	T4	7	-	-	Steep hill crest	no
25	KVLA	122	T1	9	0.122	7	Flat/shallow (<15) within 200 m	yes
26	KYMI	259	T2	11	-	-	Steep hill crest	no
27	KZN	791	-	-	0.113	6	Flat/shallow (<15) within 200 m	yes
28	LIA	67	T1	3	0.073	4	Flat/shallow (<15) within 200 m	yes
29	LKR	192	-	-	-	-	Flat/shallow (<15) within 200 m	yes
30	MGNA	58	T1	5	0.07	4	Flat/shallow (<15) within 200 m	yes
31	MHLO	175	-	-	-	-	Flat/shallow (<15) within 200 m	yes
32	NEO	510	-	-	-	-	Flat/shallow (<15) within 200 m	yes
33	NISR	44	-	-	-	-	Near cliff	no
34	NISR2	423	-	-	-	-	Near cliff	no
35	NOAC	93	T1	7	0.225	13	Flat/shallow (<15) within 200 m	yes
36	NPS	288	-	-	-	-	Flat/shallow (<15) within 200 m	yes
37	NVR	627	T1	15	0.259	15	Flat/shallow (<15) within 200 m	yes
38	ORTH	450	-	-	-	-	Flat/shallow (<15) within 200 m	yes



39	PENT	1096	-	-	-	-	-	Steep (<30) within 200 m	no
40	PLG	566	T1	5	0.073	4	-	Flat/shallow (<15) within 200 m	yes
41	PRK	130	T1	5	-	-	-	Flat/shallow (<15) within 200 m	yes
42	PSRA	13	T1	2	0.047	3	-	Flat/shallow (<15) within 200 m	yes
43	PTL	500	-	-	-	-	-	Flat/shallow (<15) within 200 m	yes
44	RDO	116	-	-	-	-	-	Flat/shallow (<15) within 200 m	yes
45	RLS	97	-	-	-	-	-	Flat/shallow (<15) within 200 m	yes
46	SIVA	96	T1	7	0.007	0	-	Flat/shallow (<15) within 200 m	yes
47	SKY	268	-	-	-	-	-	Steep (<30) within 200 m	no
48	SMG	348	T3	2	-	-	-	Flat/shallow (<15) within 200 m	yes
49	SMTH	365	T2	23	0.313	17	-	Steep (<30) within 200 m	no
50	TETR	942	-	-	-	-	-	Steep (<30) within 200 m	no
51	THERA	288	-	-	-	-	-	Steep (<30) within 200 m	no
52	THL	86	-	-	-	-	-	Flat/shallow (<15) within 200 m	yes
53	THVA	214	-	-	-	-	-	Flat/shallow (<15) within 200 m	yes
54	TNSA	21	T1	2	0.054	3	-	Flat/shallow (<15) within 200 m	yes
55	VAM	225	-	-	-	-	-	Flat/shallow (<15) within 200 m	yes
56	VLI	220	-	-	-	-	-	Flat/shallow (<15) within 200 m	yes
57	VLMS	431	T1	4	0.082	5	-	Flat/shallow (<15) within 200 m	yes
58	VLS	402	-	-	0.048	3	-	Flat/shallow (<15) within 200 m	yes
59	VLY	256	-	-	-	-	-	Flat/shallow (<15) within 200 m	yes
60	ZKR	254	T1	3	0.114	6	-	Flat/shallow (<15) within 200 m	yes

Table 5. V_{s30} estimates for the stations in this study.

340

No.	Station code	EC8 from ESM	V_{s30} from ESM (m/s)	Measured V_{s30} (Marg2021) (m/s)	Profile SiteCode (Stew2014)	V_{s30} from geology/slope proxy (Marg2021)	V_{s30} from terrain proxy (Marg2021)	Preferred V_{s30} (Marg2021)	Measured V_{s30} (HELPOS)	Potential reference site?
1	AMGA	B	502	-	-	589	475	529	-	no
2	ANKY	B	760	-	-	589	475	529	-	yes - ESM
3	APE	-	-	-	-	-	-	-	-	-
4	ARG	B	479	-	-	-	-	-	-	no
5	ASTA	B	793	-	-	538	475	506	-	yes - ESM
6	ATHP	B	453	-	-	-	-	-	975	yes - Helpos
7	DION	B	459	-	-	-	-	-	-	no
8	DLFA	A	1666	-	-	-999	475	475	-	yes - ESM
9	EVR	-	-	-	-	-	-	-	-	-
10	GVD	B	411	-	-	589	475	529	-	no
11	IACM	A	844	-	-	-	-	-	273	no
12	IDI	-	-	-	-	-	-	-	-	-
13	IKRA	-	-	-	-	589	475	529	-	no
14	IMMV	A	1036	-	-	-	-	-	-	yes - ESM
15	ITM	A	882	-	-	610	475	538	-	yes - ESM
16	JAN	B	399	-	-	589	365	464	-	no
17	KARP	A	835	-	-	-	-	-	-	yes - ESM
18	KASA	A	1006	-	-	589	475	529	-	yes - ESM
19	KEK	-	-	-	-	-	-	-	-	-
20	KLNA	B	530	-	-	371	365	368	-	no
21	KLV	-	-	-	-	-	-	-	-	-
22	KSL	B	781	-	-	137	-	137	-	yes - ESM
23	KSTE	-	-	-	-	-	-	-	-	-
24	KTHA	B	692	-	-	-	-	-	-	no
25	KVLA	B	782	-	-	528	475	501	-	yes - ESM
26	KYMI	A	844	-	-	-	-	-	-	yes - ESM
27	KZN	-	-	-	-	589	475	529	-	no
28	LIA	B	471	-	-	589	475	529	-	no
29	LKR	-	-	-	-	-	-	-	-	-



30	MGNA	B	595	-	-	589	365	464	no
31	MHLO	-	-	-	-	-	-	-	-
32	NEO	-	-	-	-	-	-	-	-
33	NISR	-	-	-	-	-	-	-	-
34	NISR2	-	-	-	-	-	-	-	-
35	NOAC	B	719	-	-	589	475	529	no
36	NPS	-	-	-	-	-	-	-	-
37	NVR	A	955	-	-	556	475	514	yes - ESM
38	ORTH	-	-	-	-	-	-	-	-
39	PENT	-	-	-	-	-	-	-	-
40	PLG	B	608	-	-	492	519	506	no
41	PRK	B	604	-	-	-	-	-	no
42	PSRA	B	412	-	-	589	497	541	no
43	PTL	-	-	-	-	-	-	-	-
44	RDO	-	-	-	-	-	-	-	-
45	RLS	-	-	-	-	-	-	-	-
46	SIVA	B	706	492	-	353	365	492	no
47	SKY	-	-	-	-	-	-	-	-
48	SMG	B	451	-	-	-	-	-	no
49	SMTH	A	1167	-	-	589	475	529	yes - ESM
50	TETR	-	-	-	-	-	-	-	-
51	THERA	-	-	-	-	-	-	-	-
52	THL	-	-	-	-	-	-	-	-
53	THVA	-	-	-	-	-	-	-	-
54	TNSA	B	401	-	-	589	475	529	no
55	VAM	-	-	-	-	-	-	-	-
56	VLI	-	-	-	-	-	-	-	-
57	VLMS	B	527	-	-	589	519	553	no
58	VLS	-	-	872	-	461	365	872	yes - Marg21
59	VLY	-	-	-	-	-	-	-	-
60	ZKR	B	522	877	-	589	519	877	yes - Marg21

Table 6. Geological conditions for the stations in this study.

No.	Station code	Geologic description - accelnet	Description (Marg2021)	Geologic Age (Marg2021)	Reference site as per Pilz et al. (2020) from EGD1	Geologic unit - this study	Geologic age - this study	Reference used - this study (HSGME map sheet or other*)	Potential reference site?
1	AMGA	Schist	Alluvial deposits	Triassic-Jurassic	-	Upper schist group (Paleogene flysch)	Middle-Upper Eocene-Oligocene	Amorgos-Donoussa Islands Sheet	yes
2	ANKY		Alluvial deposits	Upper Cretaceous	claystone	Marls, sandstones, conglomerates	Neogene (Lower Tortonian-Upper Pliocene)	Antikithira Island Sheet	likely
3	APE		-	-	Felsic rock	Metamorphic Complex	Pre-permian	Naxos Island Sheet	yes
4	ARG				-	Sgourou Formation: Marls with sand and gravel	Upper Pliocene to Pleistocene	North Rhodes	no
5	ASTA	Flysch	Alluvial deposits	Upper Eocene - Oligocene	-	Gavrovo-Tripolis Zone: Flysch mainly sandstones and conglomerates	Upper Eocene-Oligocene (?)	Astipalaia Island Sheet	no
6	ATHP	0-2m fill material/2-6m poorly cemented conglomerate/6	-	-	-	Alpine formations between the autochthonous Almyropotamos -Attiki Unit and the Pelagonian	Upper Cretaceous	Kifissia Sheet	no



		-20m very weathered sandstone/20-30m sandstone				zone (Afidnae-Tourkovounia Unit)				
7	DION		-	-	metamorphic rock (Al)	Alpine formations between the autochthonous Almyropotamos -Attiki Unit and the Pelagonian zone (Almyropotamos-Attiki autochthonous unit)	Middle Eocene	Kifissia Sheet	yes	
8	DLFA	Limestone	Alluvial deposits	Quaternary	claystone	Parnassos-Ghiona Series (limestones)	Undivined Upper Cretaceous	Delfi Sheet	yes	
9	EVR		-	-	sandstone	Pindos series (pelagic limestones)	Maestrichtian-Danian	Karpenision Sheet	yes	
10	GVD		Alluvial deposits	Jurassic - Cretaceous	-	Clays and Marls	Neogene (Middle Miocene)	Gavdos Island Sheet	no	
11	IACM		-	-	-	Marls, marly limestones, clays	Neogene (Lower-middle Pliocene)	Heraklion Sheet	likely	
12	IDI		-	-	-	Ionian Zone (Aghios Yakinthos formation)	Upper Paleocene - middle Eocene	Anoyia Sheet	yes	
13	IKRA		Alluvial deposits	Mesozoic	-	Marbles, slates	Mesozoic?	*	yes	
14	IMMV		-	-	-	Marls, sandstones, conglomerates	Quaternary older	Vatolakkos (Alikianon) Sheet	no	
15	ITM	limestone	Alluvial deposits	Quaternary - Holocene	claystone	Limestones with Rudistes	Upper Cretaceous (Santonien - Maestrichtien)	Meligalas Sheet	no	
16	JAN	limestone	Alluvial deposits	Upper Jurassic - Lower Cretaceous	-	Old alluvium with fragments of silex from Vigla limestones and Doggerian sediments	Quaternary	Ioannina Sheet	no	
17	KARP		-	-	sandstone	Tripolitza series (Flysch: Marls, sandstones and conglomerates)	Tertiary / Upper Eocen (lower Priabonian)	South Karpathos Island Sheet	yes	
18	KASA	Vigla limestone	Alluvial deposits	Upper Jurassic	limestone	Limestones of Vigla	upper Jurassic (Tithonion) - upper Cretaceous	North Korfou Sheet	yes	
19	KEK		-	-	limestone	Limestones of Vigla	upper Jurassic (Tithonion) - upper Cretaceous	North Korfou Sheet	yes	
20	KLNA	limestone/alluvial deposits	Alluvial deposits	Holocene	-	Screes and fans with calcareous material	Quaternary (Pleistocene)	Kalymnos Sheet	no	
21	KLV		-	-	-	Pindos unit (platty limestones)	Upper Cretaceous	*Trikolos (2005)	yes	
22	KSL		Alluvial deposits	Paleogene	limestone	Paxos Zone (medium-thick bedded limestones)	Paleocene	Kastellorizo Sheet	yes	
23	KSTE		-	-	-	Autochthonous series of Crete-Ionian(?) Zone (Platty limestones)	Middle Jurassic-Eocene	Mochos Sheet	yes	
24	KTHA		-	-	-	Tripolis Zone (limestones)	Cretaceous (Undivined)	Kythira Sheet	yes	
25	KVLA	limestone	Alluvial deposits	Oligocene	-	Kavala granite	Quaternary	Kavala Sheet	yes	
26	KYMI	limestone	-	-	-	Subpelagonian - Pelagonian zone (limestones transgressive)	Cenomanian - Maestrichtian	Kymi Sheet	yes	
27	KZN	limestone	Alluvial deposits	Cretaceous (Turonien-Maestrichtien)	sandstone	Pelagonian Zone (Formations of Kozani channel): calcareous material from transgression	Middle-Upper Cretaceous	Kozani Sheet	yes	



28	LIA	peridotite	Alluvial deposits	-	-	Katalakon unit (lava domes, lava flows, breccias)	Neogene (lower Miocene - Aquitanian)	Limnos (Myrina) Sheet	yes
29	LKR	limestone	-	-	limestone	Postalpine sediments (graywackes, conglomerates, quartzites, shales, sandstones)	Paleozoic (Permian - Carboniferous)	Livanatai-Atalanti Sheet	no
30	MGNA	limestone	limestones	Senonian	-	Ionian Zone (limestones with Rudist fragments)	Senonian	Kalamos Sheet	yes
31	MHLO	-	-	-	-	Scree and fans	Quaternary	Milos Island Sheet	no
32	NEO	-	-	-	-	Pelagonian Zone (Micaschists)	Preupper-Cretaceous tectonic nappe (Eohellenic tectonic nappe)	Zagora-Syki Sheet	yes
33	NISR	-	-	-	-	Andesitic lavas and pyroclastics	Quaternary	Nisyros Sheet	yes
34	NISR2	-	-	-	-	Nikia rhyolite (Domes and lava flows)	Quaternary	Nisyros Sheet	yes
35	NOAC	-	Limestone	Cretaceous (Cenomanian)	-	Allochthonous series (limestone hosting Fe-Ni pisolitic lateritic ores)	Cenomanian-Turonian	Athinai-Piraeus Sheet	yes
36	NPS	-	-	-	-	Autochthonous series of Crete-Ionian? Zone (Platty limestones)	Middle Jurassic-Eocene	Ayios Nikolaos Sheet	yes
37	NVR	sandstone	Scree and Talus Cones	Pleistocene	-	Metamorphic rocks/upper series (schists, schist-gneisses, gneisses, amphibolites and marbles)	Oligocene - Miocene	Kato Neurokopion Sheet	yes
38	ORTH	-	-	-	-	Paxos Zone limestones with Rudist fragments and Foraminifera)	Upper Cretaceous (Santonian)	Zakinthos Island Sheet	yes
39	PENT	-	-	-	sandstone	Sandstones and conglomerates of Pentalofos	Postalpine sediments (lower Miocene / Aquitanian)	Pentalofon Sheet	no
40	PLG	gneiss	Basal Conglomerate Series	Upper Miocene - Lower Pliocene	-	Quartzites and quartzitic sandstones of Svoula group	Triassic - middle Jurassic	Polygyros Sheet	yes
41	PRK	limestone	-	-	-	Extrusive Rocks (pyroclastic layer with lapilli tuff, tuff breccia or agglomerates)	Mainly Pliocene	Lesbos Island-Ayia Paraskevi Sheet	yes
42	PSRA	-	Schists	Carboniferous-Paleozoic	-	Metapelites, Phyllites, meta-litharenites, metagreywackes	Mesozoic	*Meinhold et al. (2007)	yes
43	PTL	-	-	-	-	Almyropotamos-Attiki autochthonous unit (marbles hosting Fe-mineral ore deposits)	Middle Eocene	Kifissia Sheet	yes
44	RDO	-	-	-	-	Sediments and volcanics	Upper Eocene-Oligocene	Kardamos-Sapai Sheet	yes
45	RLS	-	-	-	-	Gavrovo Zone (flysch with marls, sandstones and conglomerates)	Eocene	Nea Manolas Sheet	likely
46	SIVA	limestone	Conglomerates, sandstones, sands and marls or clays	Upper Miocene (Tortonian)	-	Series alloctones, internal zones, Asteroussia nappes (gneiss)	Upper Jurassic-Lower Cretaceous	Timbakion Sheet	yes
47	SKY	-	-	-	-	Pelagonian Zone (limestone sequence)	Middle-Upper Cretaceous	Skyros Island Sheet	yes



48	SMG	-	-	-	-	Metamorphic system (Vourliotes "Syrrachos" marbles)	Neogene	East Samos Island Sheet	yes
49	SMTH	Schist series	crumbled and symmetrically folded sedimentary rocks	Upper Jurassic/Lower Cretaceous	Ultramafic rock	Geological basement (slate series)	Upper Jurassic-Lower Cretaceous	Samothraki Sheet	yes
50	TETR	-	-	-	-	Gavrovo Zone (flysch undivided with sandstones and marls)	Priabonian-Oligocene	Mirofillon Sheet	yes
51	THERA	-	-	-	-	Prevolcanic Sedimentary, Metamorphic and Igneous Rocks (crystalline limestones)	Upper Triassic	Thira Island Sheet	yes
52	THL	Limestone	-	-	-	Pelagonian Zone (marbles)	Middle Triassic-Lower Jurassic	Farkadon Sheet	yes
53	THVA	marles	-	-	-	Conglomerates, sandstones, sands, red loams	Pleistocene	Thivai Sheet	no
54	TNSA	-	Greenschist	Permian	Felsic rock (Al)	Atticocycladic Complex, Upper unit (greenschists - prasinites)	Permian (?)	Tinos-Yaros Islands Sheet	yes
55	VAM	-	-	-	-	Marly limestone	Miocene	Chania Sheet	yes
56	VLI	-	-	-	limestone	Pelagonian Zone (carbonate rocks)	Upper Permian-Middle Triassic	Pappadhianika-Potamos Sheet	yes
57	VLMS	cretaceous limestone	Cretaceous limestone	Upper Cretaceous - Paleocene	-	Paxos Zone: limestones with Rudist fragments and Foraminifera	Upper Cretaceous (Santonian)	Zakinthos Island Sheet	yes
58	VLS	-	alluvium and scree	Holocene	-	Alluvium and scree	Holocene	Cephalonia Island (Southern Island) Sheet	no
59	VLY	-	-	-	limestone	Autochonus unit (dolomites Pirnaris)	Norian (upper Triassic) - Lias (lower Jurassic) ?	Koropi-Plaka Sheet	yes
60	ZKR	Limestone	Gray, dark-gray or black dolomite of bituminous odour when crushed	Triassic	-	Tripolitza series of Crete (limestones with Radiolites)	upper Cretaceous	Sitia (Ziros) Sheet	yes

345

4 Discussion and conclusions

In the previous, we compiled several descriptors for our stations and derived amplification characteristics from our strong-motion data analysis. We now bring everything together to co-evaluate the overall potential of our stations as reference stations. We do not attribute numerical values and weights to each parameter, as is done e.g. in the summation rationale of Lanzano et al. (2021). We believe there are inherent issues with quantifying qualitative data and treating them as homogeneous to perform mathematical operations between them. Moreover, our goal is not to provide a continuous ranking across all sites. We opt for co-assessing all input and offering an overall qualitative assessment of reference site potential. In Table 7 we consider stations that got a positive assessment in all 5 factors as 'preferred' reference sites (2 instances), those who missed 1 field as 'very good' (3 instances), and those that missed 2 fields as 'ok' (18 instances). Stations that ranked



355 lower are not recommended, though the user can select them for specific purposes or within specific frequency bands
according to her/his own judgement. Different schemes could be contrived to evaluate and even prioritise the stations, but we
do not feel an absolute grading is necessary, especially since the appropriateness will also depend on the precise nature of the
application making use of the reference motion. It is a strong message for us to convey that over half the stations did not rank
as reliable enough reference stations, and we feel that more work is needed to reassess the implications of this finding. It is
360 also interesting to note that several of our rock sites had high-frequency amplifications: this is in line with the definition of
A-class sites in EC8, which is shifting from the current version (CEN, 2004) of $V_{S30}>800$ m/s, to a new version (Labbé and
Paolucci, 2022) where there is also a provision of $f_0>10$ Hz.

In this study, we compute FAS-based HVSr for the first time for all the HL rock stations, producing f_0 and other metadata.
We also compile all existing parameters we can find from various sources (housing/installation, topography/slope, surface
365 geology, and V_{S30} ; ad-hoc Vs profiles being almost non-existent across Greek seismic rock stations). We compare and
contrast those metadata from various sources and, in addition, we offer insights and corrections based on site visits from a
network operator's point of view. We believe this operator's first-hand experience is important because geological maps
constructed at such a scale as to serve an entire country (and made by different teams, over several decades) inevitably
contain errors and simplifications, whereas a site walkover of the station location by an experienced geologist provides
370 additional reliability. Similarly, satellite-based estimates of slope/topography invariably include approximation,
homogenisation and some lack of specificity depending on the size of the 'pixel', whereas again a site visit leaves little doubt
as to the exact nature of the landscape at the exact location of the station. The information for rock stations up to now has
been sparse and scattered for the strong-motion case, and almost nonexistent for the broadband one. Until now, if a user
wished to select a reference station in the HL network, s/he might have resorted to geology, or even considered all rock
375 stations as interchangeable. We hope this work has provided the first step towards a better evaluation of rock stations and
eventually towards the better utilisation of their data.

Finally, we believe that data-derived transfer functions are extremely important and illuminating for understanding station
response. There is sometimes a fixation on V_{S30} which is not only inadequate (too shallow, and providing no indication of
impedance depth or contrast), but may even be unnecessary if we have both the geology and –what is more- the empirical
380 site response from recordings. Even a full Vs profile may be inadequate to fully assess site response, if we consider that its
high-frequency part depends heavily on the assumptions we made of damping, and –most of all- that its premise for yielding
reliable site response is that the 1D assumption holds true, which in nature is rarely the case (and especially perhaps for rock
sites - whereas empirical estimates of site effects, may have their shortcomings but reflect the 3D nature of the formations).
Our study has shown once again that not all 'rock' sites should be treated –or trusted- equally. Also, we would ask the
385 question: if we have data-derived site response, how much importance should stand-alone meta-descriptors and proxies such
as V_{S30} be given?



390

Table 7. Compilation of reference site potential per station according to all factors and final disposition.

No.	Station code	Topography	V _{s30}	Geology	HV shape & level	Directionality	Final disposition
1	AMGA	yes	no	yes	yes		ok
2	ANKY	yes	yes - ESM	likely	no	yes	
3	APE	yes	-	yes	no		
4	ARG	yes	no	no	ok		
5	ASTA	yes	yes - ESM	no	yes		ok
6	ATHP	yes	yes - Helpos	no	yes		ok
7	DION	yes	no	yes	ok		
8	DLFA	no	yes - ESM	yes	yes	yes	very good
9	EVR	yes	-	yes	yes		ok
10	GVD	yes	no	no	no	yes	
11	IACM	yes	no	likely	no		
12	IDI	no	-	yes	yes	yes	ok
13	IKRA	yes	no	yes	ok		
14	IMMV	yes	yes - ESM	no	yes		ok
15	ITM	yes	yes - ESM	no	ok		
16	JAN	yes	no	no	ok		
17	KARP	no	yes - ESM	yes	yes	yes	very good
18	KASA	no	yes - ESM	yes	yes		ok
19	KEK	no	-	yes	ok		
20	KLNA	yes	no	no	no		
21	KLV	no	-	yes	yes	yes	ok
22	KSL	no	yes - ESM	yes	ok		
23	KSTE	no	-	yes	ok		
24	KTHA	no	no	yes	no		
25	KVLA	yes	yes - ESM	yes	yes	yes	preferred
26	KYMI	no	yes - ESM	yes	ok		
27	KZN	yes	no	yes	ok		
28	LIA	yes	no	yes	ok		
29	LKR	yes	-	no	no		
30	MGNA	yes	no	yes	yes		ok
31	MHLO	yes	-	no	no		
32	NEO	yes	-	yes	no		
33	NISR	no	-	yes	no		
34	NISR2	no	-	yes	no		
35	NOAC	yes	no	yes	ok		
36	NPS	yes	-	yes	yes		ok
37	NVR	yes	yes - ESM	yes	ok	yes	preferred
38	ORTH	yes	-	yes	no		
39	PENT	no	-	no	yes		
40	PLG	yes	no	yes	yes	yes	ok
41	PRK	yes	no	yes	no		
42	PSRA	yes	no	yes	no	yes	ok
43	PTL	yes	-	yes	yes		ok
44	RDO	yes	-	yes	ok		
45	RLS	yes	-	likely	ok		
46	SIVA	yes	no	yes	no		
47	SKY	no	-	yes	no		
48	SMG	yes	no	yes	no		
49	SMTH	no	yes - ESM	yes	yes		ok
50	TETR	no	-	yes	no		
51	THERA	no	-	yes	yes		
52	THL	yes	-	yes	yes	yes	very good
53	THVA	yes	-	no	no		
54	TNSA	yes	no	yes	yes		ok
55	VAM	yes	-	yes	ok		
56	VLI	yes	-	yes	no	yes	ok
57	VLMS	yes	no	yes	no		
58	VLS	yes	yes - Marg21	no	yes		ok
59	VLY	yes	-	yes	ok		



60 ZKR yes yes - Marg21 yes no ok

Data availability

395 All waveforms and station metadata were downloaded and are freely accessible at <https://eida.gein.noa.gr/>, the regional node
of EIDA (the European Integrated Data Archive) hosted by the Institute of Geodynamics of the National Observatory of
Athens (NOA). Data from NOA's seismic network bear the network code HL and are attributed DOI:10.7914/SN/HL. Event
parameters come from the seismic catalogue of NOA, freely accessible here: <https://eida.gein.noa.gr/fdsnws/availability/1>.
Station metadata come from the various articles cited in the paper, as well as the ESM (<https://esm-db.eu/>; Lanzano et al.,
400 2021; Luzi et al., 2016). Maps published by the Hellenic Survey of Geology and mineral Exploration are generally available
by HSGME for purchase and hence not freely accessible.

Author contribution

OJK had the idea, coordinated the team, and wrote the paper. AP performed manual data processing and final data check and
curated the database. EVP performed the main coding and calculations. ZC compiled and interpreted the ground motion
405 station metadata. FG performed manual data processing. SL contributed the geological interpretations and oversaw PS and
KF in compiling the geological station metadata. CPE provided insights on station history, installation and performance.

Competing interest

The contact author has declared that none of the authors has any competing interests.

Acknowledgements

410 Discussions with several colleagues have helped the lead author since she joined NOA in 2018; among others, Ioannis
Kalogeras, Thymios Sokos, Hiroshi Kawase, Laurentiu Danciu and Alexis Chatzipetros are cordially thanked in order of
appearance. No funding is acknowledged, except the small internal scholarship 'ROAR' awarded by NOA to OJK. Some
plots were created using Generic Mapping Tools (GMT; Wessel et al. 2013) and the help of this fantastic tool is cordially
acknowledged. Finally, no AI was used in developing this manuscript; we used what human intelligence was available.



415 **References**

- Ancheta, T.D., R.B. Darragh, J.P. Stewart, E. Seyhan, W.J. Silva, B.S.-J. Chiou, K.E. Wooddell, R.W. Graves, A.R. Kottke, D.M. Boore, T. Kishida, J.L. Donahue, NGA-West2 Database, *Earthquake Spectra*, 30(3), 989–1005. doi: <https://doi.org/10.1193/070913EQS197M>, 2014.
- Ashford, S.A. and Sitar N.: Analysis of Topographic Amplification of Inclined Shear Waves in a Steep Coastal Bluff, *Bull. Seism. Soc. Am.*, 87, 692-700, DOI: [10.1785/BSSA0870030692](https://doi.org/10.1785/BSSA0870030692), 1997.
- Borcherdt, R. D.: Effects of local geology on ground motion near San Francisco Bay, *Bull. Seismol. Soc. Am.*, 60, 29–61, 1970.
- Brune, J.N.: Tectonic stress and the spectra of seismic shear waves from earthquakes, *J. Geoph. Res.*, 75, 4997–5002, 1970.
- Brune, J.N.: Correction to ‘Tectonic stress and the spectra, of seismic shear waves from earthquakes, *J. Geoph. Res.*, 76, 5002, 1971.
- CEN (Comité Européen de Normalisation): Eurocode 8: Design of structures for earthquake resistance. Part 1: general rules, seismic actions and rules for buildings (EN 1998–1: 2004), Brussels, Belgium, 2004.
- Cultrera, G., Cornou, C., Di Giulio, G. and Bard, P.Y.: Indicators for site characterization at seismic station: recommendation from a dedicated survey, *Bull. Earth. Eng.* 19 (11), 4171-4195, DOI: [10.1007/s10518-021-01136-7](https://doi.org/10.1007/s10518-021-01136-7), 2021.
- 430 Di Giulio, G., Cultrera, G., Cornou, C., Bard, P.Y., Tfaily, B.Al.: Quality assessment for site characterization at seismic stations, *Bull. Earth. Eng.*, 19 (12), 4643-4691, doi: [10.1007/s10518-021-01137-6](https://doi.org/10.1007/s10518-021-01137-6), 2021.
- Evangelidis, C.P., Triantafyllis, N., Samios, M., Boukouras, K., Kontakos, K., Ktenidou, O-J. and 32 others: Seismic waveform data from Greece and Cyprus: Integration, archival and open access, *Seismol. Res. Letts*, 92, 1672–1684, doi: [10.1785/0220200408](https://doi.org/10.1785/0220200408), 2021.
- 435 Geli, L., Bard P.Y. and Jullien B.: The effect of topography on earthquake ground motion: a review and new results. *Bull. Seism. Soc. Am.* 78, 42-63, 1988.
- Goulet, C., Kishida, T., Ancheta, T.D., Cramer, C.H., Darragh, R.B., Silva, W.J., Hashash, Y.M.A., Harmon, J., Stewart, J.P., Wooddell, K.E. and Youngs, R.R.: PEER NGA-East database. PEER Report 2014/17, Berkeley, CA: Pacific Earthquake Engineering Research Center, 2014.
- 440 Grendas, I., Theodoulidis, N., Hatzidimitriou, P., Margaris, B. and Drouet, S.: Determination of source, path and site parameters based on non-linear inversion of accelerometric data in Greece, *Bull. Earth. Engin.*, doi: [10.1007/s10518-018-0379-8](https://doi.org/10.1007/s10518-018-0379-8), 2018.
- Ito, E., Nakano, K., Nagashima, F. and Kawase H.: A Method to Directly Estimate S-Wave Site Amplification Factor from Horizontal-to-Vertical Spectral Ratio of Earthquakes (eHVSRS), *Bull. Seismol. Soc. Am.*, 110, 2892–2911, doi: [10.1785/0120190315](https://doi.org/10.1785/0120190315), 2020.
- 445



- Kishida, T., Ktenidou, O.-J., Darragh, R. and Silva, W.: Semi-automated procedure for windowing time series and computing Fourier Amplitude Spectra (FAS) for the NGA-west2 database. PEER report 2016/02, Berkeley, CA: Pacific Earthquake Engineering Research Center, 63, 2016.
- Konno, K. and Ohmachi, T.: Ground-motion characteristics estimated from spectral ratio between horizontal and vertical components of microtremor. *Bull. Seismol. Soc. Am.*, 88(1), 228–241, <https://doi.org/10.1785/BSSA0880010228>, 1998.
- 450 Ktenidou, O.-J. and Abrahamson, N.: Empirical estimation of high-frequency ground motion on hard rock. *Seismol. Res. Letts*, 87, 1465–1478, [DOI: 10.1785/0220160075](https://doi.org/10.1785/0220160075), 2016.
- Ktenidou, O.-J., Kalogeras, I.: The accelerographic network of the National Observatory of Athens, Greece: improving site characterisation using strong motion recordings, 2nd International Conference on Natural Hazards & Infrastructure (ICONHIC), Chania, 23-26 Jun, 2019.
- 455 Ktenidou, O.-J.: Hard as a rock? Reconsidering rock-site seismic response and reference ground motions. In: *Progresses in European Earthquake Engineering and Seismology - Third European Conference on Earthquake Engineering and Seismology – Bucharest, 2022*, Ed. R. Vacareanu & C. Ionescu, Springer Proceedings in Earth and Environmental Sciences, https://doi.org/10.1007/978-3-031-15104-0_3, 2022.
- 460 Ktenidou, O.-J., Chávez-García, F.J., Raptakis, D. and Pitilakis, K.D.: Directional dependence of site effects observed near a basin edge at Aegion, Greece, *Bull. Earth. Eng.*, 14(3), 623-645, [doi:10.1007/s10518-015-9843-x](https://doi.org/10.1007/s10518-015-9843-x), 2016.
- Ktenidou, O.-J., Gkika, F. and Evangelidis, C.: The Quest for Rock Site Characterization for the Greek National Seismic Network, EUROENGE0: 3rd European Regional Conference of IAEG, Athens/online, 6-9 Oct, 2021a.
- Ktenidou, O.-J., Gkika, F., Pikoulis, E.V. and Evangelidis, C.: Hard as a rock? Looking for typical and atypical reference sites in the Greek network, EGU General Assembly (online), 19-30 Apr., [DOI:10.5194/egusphere-egu21-13659](https://doi.org/10.5194/egusphere-egu21-13659), 2021b.
- 465 Labbé, P. and Paolucci, R.: Developments Relating to Seismic Action in the Eurocode 8 of Next Generation. In: *Progresses in European Earthquake Engineering and Seismology - Third European Conference on Earthquake Engineering and Seismology – Bucharest, 2022*, Ed. R. Vacareanu & C. Ionescu, Springer Proceedings in Earth and Environmental Sciences, 2022.
- 470 Lanzano, G., Luzi, L., Cauzzi, C., Bienkowski, J., Bindi, D., Clinton, J., Cocco, M., D’Amico, M., Douglas, J., Faenza, L., Felicetta, C., Galovic, F., Giardini, D., Ktenidou, O.-J. and 12 others: Accessing European Strong-Motion Data: An Update on ORFEUS Coordinated Services, *Seismol. Res. Letts* 92, 1642–1658, [doi:10.1785/0220200398](https://doi.org/10.1785/0220200398), 2021.
- Lanzano, G., Felicetta, C., Pacor, F., Spallarossa, D. and Traversa, P.: Methodology to identify the reference rock sites in regions of medium-to-high seismicity: An application in Central Italy, *Geophys. J. Int.*, 222, 3, 2053–2067, [DOI: 10.1093/gji/ggaS261](https://doi.org/10.1093/gji/ggaS261), 2020.
- 475 Lanzano, G., Felicetta, C., Pacor, F., Spallarossa, D. and Traversa, P.: Generic-To-Reference Rock Scaling Factors for Seismic Ground Motion in Italy, *Bull. Seismol. Soc. Am.* XX, 1–24, [doi: 10.1785/0120210063](https://doi.org/10.1785/0120210063), 2022.
- Lermo, J., and Chavez-Garcia, F.G.: Site effect evaluation using spectral ratios with only one station, *Bull. Seismol. Soc. Am.*, 83, 1574–1594, 1993.



- 480 Luzi, L., Puglia, R., Russo, E., D'Amico, M., Felicetta, C., Pacor, F., Lanzano, G., Çeken, U., Clinton, J., Costa, G., Duni, L., Farzanegan, E., Gueguen, P., Ionescu, C., Kalogeras, I., Özener, H., Pesaresi, D., Sleeman, R., Strollo, A. and Zare, M.: The engineering strong motion database: A platform to access pan-European accelerometric data, *Seismol. Res. Letters*, 87(4), 987–99, DOI: [10.1785/0220150278](https://doi.org/10.1785/0220150278), 2016.
- Margaris, B.E., Scordilis, M., Stewart, J.P., Boore, D.M., Theodoulidis, N., Kalogeras, I., Melis, N., Skarlatoudis, A., Klimis, 485 N. and Seyhan, E.: Hellenic strong-motion database with uniformly assigned source and site metadata for period of 1972–2015, *Seismol. Res. Letts*, 92, 2065–2080, doi: [10.1785/0220190337](https://doi.org/10.1785/0220190337), 2021.
- Margaris, B., Kalogeras, I., Papaioannou, Ch., Savvaidis, A. and Theodoulidis, N.: Evaluation of the national strong motion network in Greece: Deployment, data processing and site characterization, *Bull. Earth. Engin.*, 12, 237–254, <https://doi.org/10.1007/s10518-013-9580-y>, 2014.
- 490 Meinhold, G., D. Kostopoulos, T. Reischmann: Geochemical constraints on the provenance and depositional setting of sedimentary rocks from the islands of Chios, Inousses and Psara, Aegean Sea, Greece: implications for the evolution of Palaeotethys. *Journal of the Geological Society*, 164 (6), 1145–1163. doi: <https://doi.org/10.1144/0016-76492006-111>, 2007
- Pilz, M., Cotton, F. and Reddy Kotha, S.: Data-driven and machine learning identification of seismic reference stations in Europe, *Geoph. J. Int.*, 222, 2, 861–873, <https://doi.org/10.1093/gji/ggaa199>, 2020.
- 495 Puglia, R., Albarello, D., Gorini, A., Luzi, L., Marcucci, S. & Pacor, F. Extensive characterization of Italian accelerometric stations from single-station ambient-vibration measurements, *Bull. Earthq. Eng.*, 9, 1821–1838, <https://doi.org/10.1007/s10518-011-9305-z>, 2011.
- Silva, W.J. and Darragh, R.: Engineering Characterization of Earthquake Strong Ground Motion Recorded at Rock Sites (TR-102261), Palo Alto, CA: Electric Power Research Institute. Available at: [https://www.epri.com/research/products/TR-](https://www.epri.com/research/products/TR-102262) 500 [102262](https://www.epri.com/research/products/TR-102262), 1995.
- Steidl, J.H., Tumarkin, A.G. and Archuleta, R.J: What is a reference site? *Bull. Seism. Soc.Am.*, 86(6), 1733–1748, DOI: [10.1785/BSSA0860061733](https://doi.org/10.1785/BSSA0860061733), 1996.
- Stewart, J.P., Klimis, N., Savvaidis, A., Theodoulidis, N., Zargli, E., Athanasopoulos, G., Pelekis, P., Mylonakis, G. and Margaris, B.: Compilation of a local VS profile database and its application for inference of VS30 from geologic and 505 terrain-based proxies, *Bull. Seism. Soc. Am.*, 104, 2827–2841, <https://doi.org/10.1785/0120130331>, 2014.
- Theodoulidis, N., Kalogeras, I., Papazachos, C.B., Karastathis, V., Margaris, B.N., Papaioannou, Ch., Skarlatoudis A.A.: HEAD v1.0: A unified Hellenic Accelerogram Database, *Seis. Res. Lett.*, 75, 36–45, 2004.
- Trikolas, C.J. Geological map of Aigion area ‘Aigion sheet’. National Technical University of Athens, Faculty of Mining Engineering and Metallurgy, Section of Geological Sciences, 2005.
- 510 Van Houtte, C., Ktenidou, O.-J., Larkin, T. and Kaiser, A.: Reference stations for Christchurch, *Bulletin of the New Zealand Soc. Earth. Eng.*, 45(4), 184–195, doi:[10.5459/bnzsee.45.4.184-195](https://doi.org/10.5459/bnzsee.45.4.184-195), 2012.



Wessel, P., Smith, W., Scharroo, R., Luis, J. and Wobbe, F.: Generic mapping tools: improved version released, Eos Trans. AGU, 94(45), 409–410, 2013.